International Journal of High-Rise Buildings
December 2020, Vol 9, No 4, 325-334
https://doi.org/10.21022/IJHRB.2020.9.4.325

International Journal of
High-Rise Buildings
www.ctbuh-korea.org/ijhrb/index.php

Interfacial Stress Concentrations of Vertical Through-plate to H-beam Connections in CFT Column

Insub Choi[1], HakJong Chang[1], and JunHee Kim[1]

[1]*Department of Architectural and Architecture Engineering, Yonsei University, Seoul 03722, Korea*

Abstract

This paper aims to evaluate the interfacial stress concentrations on connection between vertical through-plate and H-beam in CFT column. Full-scale experiments were performed on three specimens with varying thickness of the vertical through-plate to investigate the interfacial stress concentration factor in the connections. The specimens underwent brittle failure at the location where the steel beam is connected to the vertical through-plate before the steel beam reached its plastic moment. The strain data of the part were analyzed, and the sectional analyses were conducted to determine appropriate residual stress models. In addition, the stress concentration factor was quantified by comparing the analytical local behavior in which the stress concentration is not reflected and the experimental data reflecting the stress concentration. The results showed that the maximum reduction of the stress concentration factor due to an increase in the thickness of the vertical through-plate is 50.3%.

Keywords: Interfacial stress concentration, Vertical through-plate, Thermally-induced initial damage, Concrete-filled steel tube, Residual stress

1. Introduction

Concrete-filled steel tube (CFT) columns are steel-concrete composites that combine the high tensile force and ductility of steel with the high compression resistance and stiffness of concrete (Sakino *et al*. 2004). CFT columns consist of a circular or box-type steel tube filled with plain or reinforced concrete. The composite actions of these two different materials can greatly increase sectional performance (Choi *et al*. 2015, 2016; Kim and You 2015). Since the introduction of CFT column-supported buildings in 1902 by Sewell (Sewel 1902), CFT columns have been used in various structures, such as high-rise buildings (Samarakkody *et al*. 2017), offshore structures (Chen *et al*. 2017), and bridges (Xiao *et al*. 2011). Previous studies on the CFT columns (Gupta and Singh 2014; Hajjar *et al*. 1998; Kuranovas and Kvedaras 2007; Srinivasan and Schneider 1999; Young and Ellobody 2006) have shown that they have a high load-bearing capacity, are economically sound, and are smaller sections than alternative types of columns. However, significant amounts of interfacial stress concentration are likely to occur where CFT columns and steel beams are welded together (Chan *et al*. 2010), so panel zones need to be adequately reinforced to reduce the interfacial stress concentrations (Huang *et al*. 2002).

Horizontal diaphragms are generally installed on CFT columns in a direction parallel to the flanges of steel beams to reduce the interfacial stress concentrations. The three types of horizontal diaphragms are internal diaphragms, external diaphragms, and through diaphragms (Qin *et al*. 2014c). Qin *et al*. (2014a) conducted a cyclic test to evaluate the behavior of CFT column panel zones reinforced with internal diaphragms and reported that steel beam flanges suffered fractures due to interfacial stress concentrations in the tapered plate attached to the end of the steel beam flanges. External diaphragms are easier to construct than internal diaphragms, but interfacial stress concentrations are likely to occur at the connection between the CFT column and the steel beam, so these connections are reinforced with steel plates (Lee *et al*. 2010). Through diaphragms reduce the interfacial stress concentrations on the connections between steel beams and CFT columns (Qin *et al*. 2014b). However, they are more challenging to install in-situ because they require additional plates in steel beam flanges.

The interfacial stress concentrations at the connections between CFT columns and steel beams can be analyzed through numerical modeling or experiments. The behavior of the connections between CFT columns and steel beams can be evaluated using an analytical model (Kang *et al*. 2014) or a hybrid model that combines analytical and informational models (Kim *et al*. 2010; Kim *et al*. 2012). However, no existing models evaluate the behavior of the connections between CFT columns with diaphragms and steel beams, so these connections are generally analyzed experimentally. Chen *et al*. (2004) experimentally showed that reinforcing rib plates on the upper part of steel beam

†Corresponding author: Kim, JunHee
Tel: +82-2-2123-7469, Fax: +82-2-365-4668
E-mail: junhkim@yonsei.ac.kr

flanges reduces the interfacial stress concentrations on their connections with CFT columns with internal diaphragms. Choi *et al*. (2008) proposed a combined-cross diaphragm that combines internal and external diaphragms. The experimental results demonstrated that the combined-cross diaphragm could reduce the interfacial stress concentration on the connections. Kim *et al*. (2008) and Shin *et al*. (2004) showed that installing vertical plates at the corners of box-type CFT columns with external diaphragms reduced the interfacial stress concentrations on their connections with steel beams. These studies showed that reinforcing horizontal diaphragms with additional plates reduced the interfacial stress concentrations on the connections between CFT columns and steel beams. However, installing additional plates exacerbates the concrete filling problems of CFT columns with diaphragms installed horizontally.

An alternative to installing diaphragms horizontally is to install steel plates vertically in CFT columns, which connect diaphragms and steel beams (Mirghaderi *et al*. 2010; Torabian *et al*. 2012; Zeinizadeh Jeddi *et al*. 2017). These vertical plates penetrate the CFT column, so their structural behavior is similar to that of the through diaphragms. These plates can reduce the interfacial stress concentrations on the connections between CFT columns and steel beams because the connections between vertical plates and the steel beams were located away from the CFT columns' surface. However, the steel plates are inserted through the corner of the box-type columns, making it difficult to connect them with steel beams. These vertical plates have the advantage of reducing the severity of the concrete filling problems that occur when using horizontal diaphragms, as mentioned above. Therefore, this study seeks to evaluate the interfacial stress concentration of connections with vertical through-plates, simplified the construction process than existing vertical plates.

In this study, the interfacial stress concentrations on connections between vertical through-plates and H-beam in CFT columns were evaluated through experiments and analysis. The independent variable in the experiment was the thickness of the vertical through-plates. Experiments were conducted on three full-scale specimens to investigate the interfacial stress concentration. Based on the interfacial stress concentrations on the connections, an analytical model was developed that reflects initial thermal damage caused by welding the connections. In addition, the stress concentration factor (SCF) on the connections were quantitatively analyzed using an analytical model according to the thickness of the vertical through-plates.

2. Experimental test

2.1. Full-scale Test Specimens

The full-scale experiments were conducted to investigate the interfacial stress concentration of vertical through-plate to H-beam connections in the CFT column, as shown in Figure 1. The CFT column sections were 400 mm × 400 mm and 3000 mm long. The steel beam sections were H-700 mm × 300 mm × 13 mm × 24 mm and 3200 mm long. Five holes with diameters of 30 mm were drilled at 100 mm intervals on the upper flanges 50 mm away from the beam ends to connect an actuator. The vertical through-plates used to connect the CFT columns and H-beams were a width of 400 mm and a height of 350 mm. Three specimens were manufactured with the three different thicknesses of the vertical through-plate of 40 mm, 45 mm, and 50 mm.

The connection details of the specimens are summarized in Figure 2. The construction procedure of the specimens consists of the following three steps; (i) fabrication of

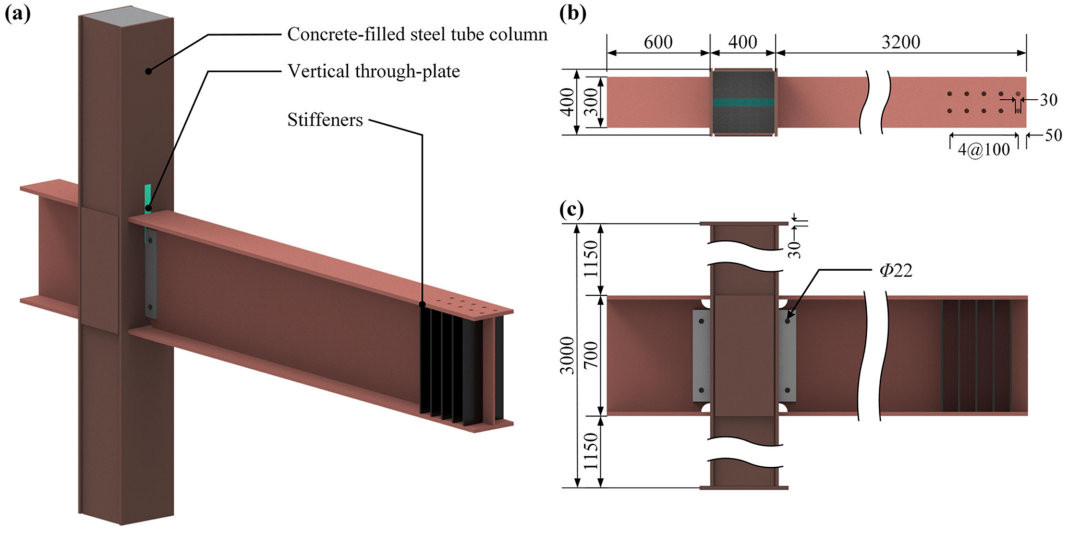


Figure 1. Dimensions of test specimens for the CFT column to H-beam connections reinforced with vertical through-plate: (a) outline; (b) plan view; (c) side view (unit in mm).

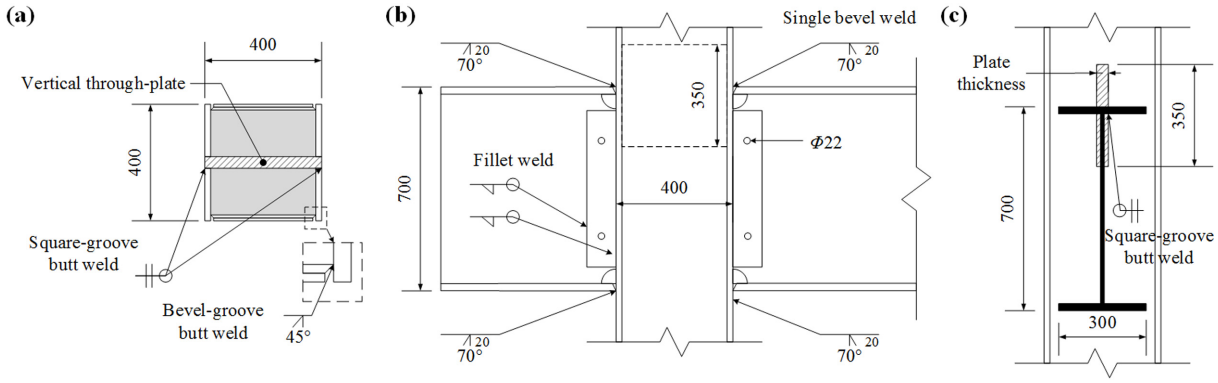


Figure 2. Details of welded connections of the CFT column to H-beam connections: (a) CFT column to vertical through-plate; (b) CFT column to H-beam; (c) vertical through-plate to H-beam (unit in mm).

CFT column, (ii) installation of vertical through-plate into the CFT column, and (iii) construction of the connection between H-beam and vertical through-plate, CFT column. First, the CFT columns were fabricated by joining two 20 mm- and two 10 mm-thick steel plates by a bevel-groove butt weld at a 45º angle as shown in Figure 2(a). A 350 mm-long hole was punched in both steel plates of the CFT columns depending on the thickness of the vertical through-plates. Second, the vertical through-plates were inserted into the pre-punched holes of the CFT columns then the four sides where the two elements met were connected by square-groove butt welds as shown in Figure 2(a). Third, single bevel welds directly connected the center of the upper flanges of the beam and the vertical through-plates at a 70º angle as shown in Figure 2(b). Other parts of the flange except for the center of the upper flange were welded to the CFT column by a 70º angle single bevel weld. The webs of the beams and the CFT columns were connected by two 10 mm-thick plates with fillet welds and two bolts with diameters of 22 mm. The connections of the vertical through-plates to the beams are shown in Figure 2(c). The CFT column, the vertical through-plates, and the upper flange were all welded together at the connections, which are likely to generate excessive heat induced by the welding process. Therefore, there is a possibility that thermally-induced initial damage such as residual stress occurs in the corresponding parts resulted from an uneven cooling process.

The grade of all of the steel materials used in the specimens was SM490A. According to the Korean standard of rolled steel for welded structures (KS D 3515) (KATS 2014), the yield strength and tensile strength of SM490A steel are 315 MPa and 490 MPa, respectively. A series of the coupon test was conducted, and the results of the coupon test showed that the yield strength and tensile strength were 381 MPa and 550 MPa, respectively. The strength of the steel materials used in the specimens satisfied the lower limits specified by the standard. The material strengths observed during the coupon tests were used in the sectional analysis (Section 4).

2.2. Experiment Setup and Process

Figure 3 shows the experimental setup with the boundary conditions. An oil jack with a capacity of 1000 kN was connected to the end of the beam 2950 mm away from the welded connection using pre-drilled holes to simulate gravity load. A displacement-controlled load with a 0.2 mm/sec rate was imposed on the experimental specimens using the oil jack. Five 12 mm-thick vertical stiffeners were installed at 100 mm intervals on the beams' webs located below the oil jack to prevent local buckling in the beam. Two hinges were installed at both ends of the CFT columns to simulate their ideal boundary conditions.

Six strain gauges were installed on the upper flanges of the beams to measure the interfacial stress concentrations on the welded connections between the vertical through-plates and H-beams (Figure 4). Long *et al*. (2009) reports that there is no residual stress induced by welding in part 90 mm or more away from the welded connection. Thus, line A was made 120 mm away from the welded con-

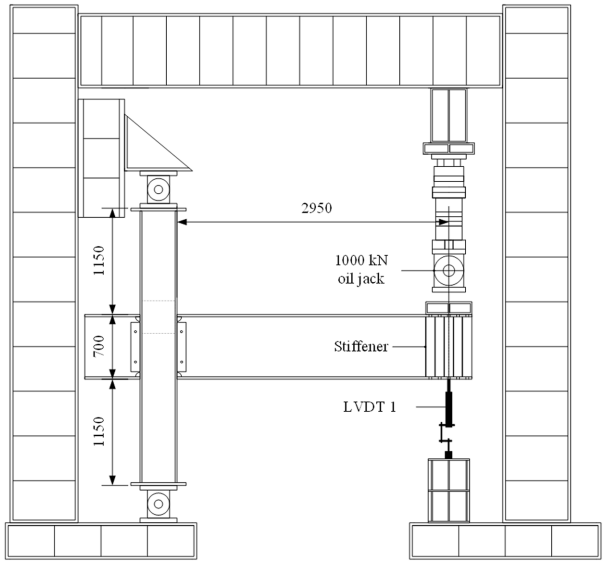


Figure 3. Diagram of the monotonic test setup (unit in mm).

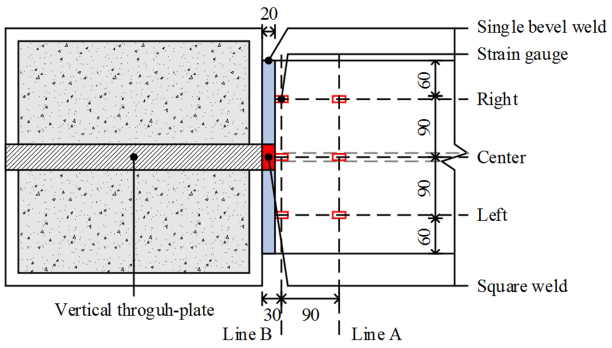


Figure 4. Locations of the strain-measuring devices (strain gauges) in the upper flange near the welded connection (unit in mm).

nection to avoid the thermally-induced initial damage in this experiment. Line B was made 30 mm away from the welded connection to measure the experimental strain that reflects the thermally-induced initial damage. The strain measured in line A and line B were used to derive the moment-strain curve representing the local behavior of the specimens.

3. Experimental Investigation of Interfacial Stress Concentration

3.1. Moment-strain Behavior of Connections

All specimens underwent premature failure in the connections between vertical through-plate and steel beam before they reached the steel beam's plastic moment. The premature failures occurred due to interfacial stress concentrations occurring at the connection between the vertical through-plates and steel beams. So, local behaviors were analyzed using the strain data to determine whether the interfacial stress concentrations occur at the center of the flange, where the vertical through-plates and steel beams were connected. As shown in Figure 5, the moment-strain curves for the different strain measurement locations were compared to analyze the interfacial stress concentrations on the connection between the vertical through-plates and steel beams. The x-axis and y-axis represent the normalized yield strain and yield strength, respectively. In the graph, the analytical curve was derived using equation (1) and then represented by normalized yield strain and yield strength. The yield strain and the yield strength of the steel beams derived from the material test results were 1856×10^{-6} and 2118.4 kNm, respectively.

$$M=\frac{EI}{y}\varepsilon=K\varepsilon \tag{1}$$

Where M is the bending moment (kNm), E is the initial modulus (205,000 MPa), I is the moment of inertia (2.01E-03 m^4), and y is the distance from the neutral axis to the end of the flange (0.35 m).

A comparison of the normalized moment-normalized strain curves for each strain measurement position showed that the flange of the steel beams (line A) maintained linear behavior until reaching their maximum strength. In the case of the welded connections (line B), the left and right flanges connected to the CFT columns maintained linear behavior, except for the DT-45 specimen, until reaching the maximum strength. In all specimens, the center of the flange, which is the connection of the vertical through-plate and the steel beam, suffered yielding without maintaining the linear behavior. As stress became concentrated on the connections between the vertical through-plates and steel beams, fractures occurred in the connections before the entire sections of the steel beams reached their plastic regions. In order to analyze the effect of interfacial stress concentrations on the local behavior of the welded connections, the experimental initial stiffness of the specimens is compared with the analytical initial stiffness.

3.2. Initial Stiffness of Connections

In Figure 5, the initial stiffness, as represented by the slope, was proportional to the *EI/y* of the steel beam, and the analytical initial stiffness was 1. The *E*, *I,* and *y* values of the steel beams did not vary by the thickness of the vertical through-plates, so in the absence of interfacial stress concentrations, the steel beams would be expected to have the same experimental initial stiffness values for all flange measurement positions, namely the center, left side, and right side. Figure 6 shows the experimental initial stiffness derived from the normalized moment-normalized strain curve for each specimen according to the strain measurement positions. The experimental initial stiffness of the steel beams ranged from 0.931 to 1.132, which were close to 1 (i.e., the analytical initial stiffness). The experimental initial stiffness for the left and right sides connected to the CFT columns ranged from 1.040 to 1.240, which were close to 1. However, the experimental initial stiffness for the center connected to the vertical through-plates ranged from 0.434 to 0.549, which were considerably lower than the analytical initial stiffness.

The early yielding of the connections between the vertical through-plates and steel beams was likely related to their low initial stiffness. After early yielding occurred due to the thermally-induced initial damage to the connection, the interfacial stress concentrations on the center of the connections contributed significantly to the premature failure of the specimens. The initial stiffness of the specimens was positively correlated with the thickness of the vertical through-plates. Therefore, it was experimentally found that using a thicker vertical through-plate has a favorable effect of alleviating the interfacial stress concentration in the connection between the vertical through-plate and the steel beam.

The initial stiffness is determined by the *EI/y* value, so the moment-strain curve shows the initial modulus (*E*) of the center of the flanges connected with the vertical through-plates was reduced due to early yielding. This

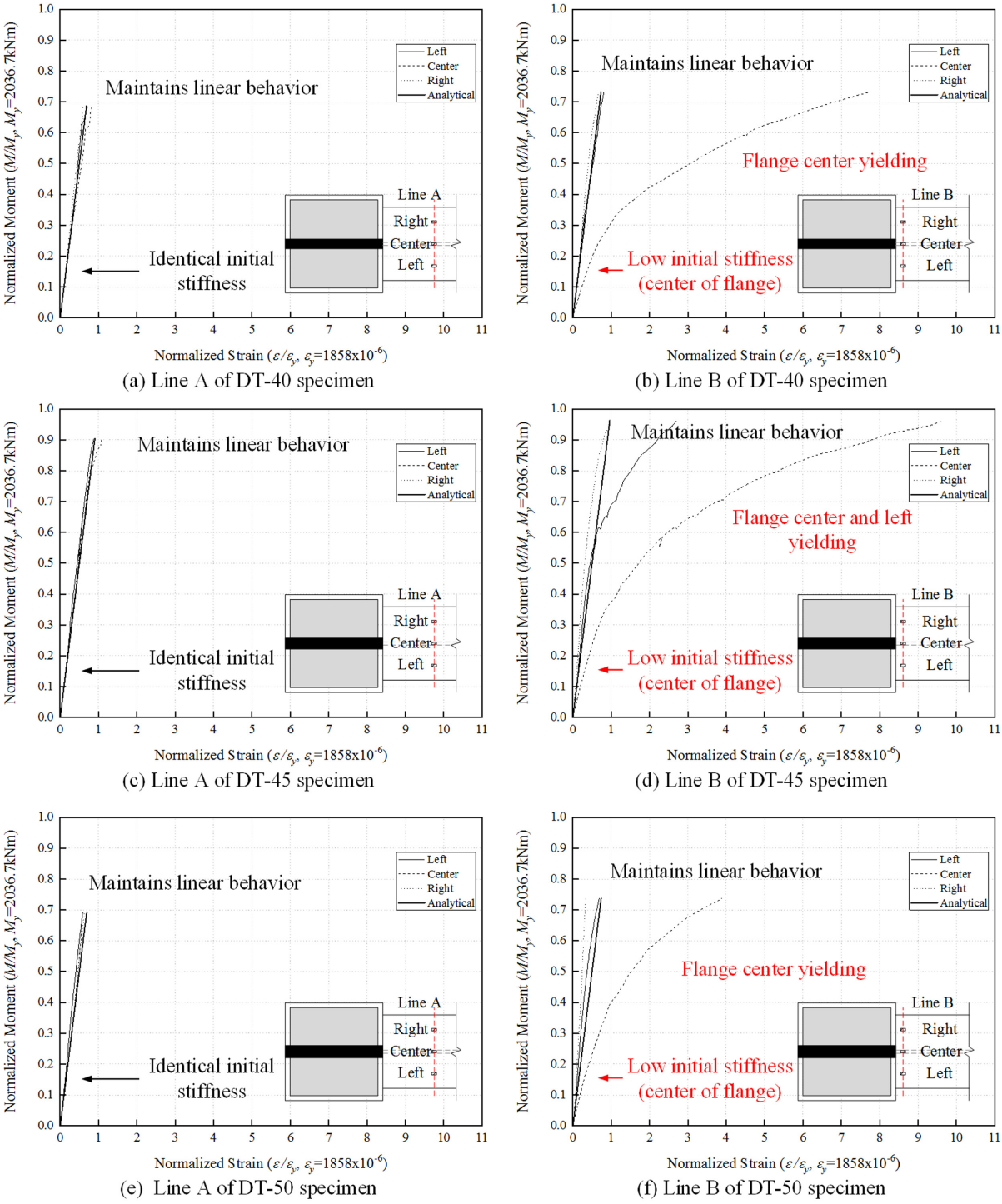


Figure 5. Local moment-strain curve of beam element (line A) and welded connection (line B).

result was a product of the fact that the *I* and *y* values are determined by the geometry of the beam section and are constant regardless of the strain measurement position. However, the thermally-induced initial damage can increase strain by deforming the steel [34,35], reducing the *E* value, as shown in this experiment. There is no noticeable decrease in the *E* value on either the left or right sides of the connections to the CFT columns in either line A, which represents the behavior of the steel beams, or line B, which represents the behavior of the connections. However, the *E* value decreased by 43.4-54.9% due to early yielding resulting from thermally-induced initial damage in the connection between the vertical through-plates and steel beams. Therefore, early yielding caused by the thermally-induced initial damage increased interfacial stress concentrations and significantly increased the

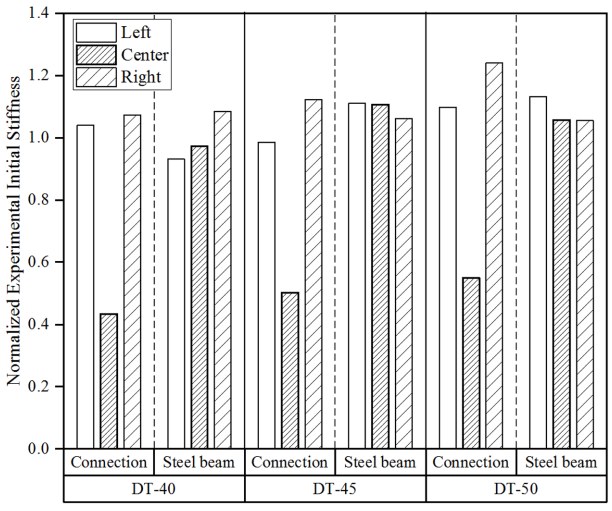


Figure 6. Comparison of normalized experimental initial stiffness for the test specimens according to the measuring locations.

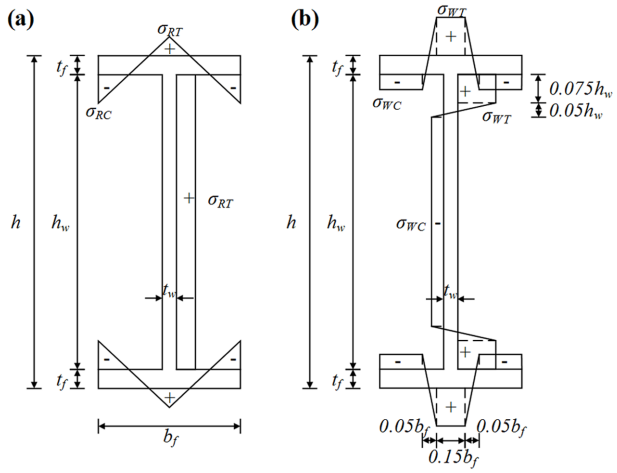


Figure 7. Residual stress models to consider the thermally-induced initial damages: (a) Galambos and Ketter model for hot-rolling (Galambos and Ketter 1959); (b) ECCS model for welding and hot-rolling (ECCS 1976).

likelihood of premature failure. Details on the interfacial stress concentrations given the thermally-induced initial damage are discussed in Section 4.

4. Interfacial Stress Concentration on Connections Induced by Initial Damages

This section discusses the interfacial stress concentrations on connections between the vertical through-plates and H-beams in the CFT columns. The experimental results showed that early yielding due to the thermally-induced initial damage significantly increased interfacial stress concentrations. In this regard, the thermally-induced initial damages are considered as residual stress models for hot-rolling and welding through literature reviews (Abambres and Quach 2016; Yang *et al*. 2016; Young and Schulz 1977). Analytical moment-strain curves were derived through sectional analyses with residual stress models, then yield strength and yield strain were evaluated to determine an appropriate residual stress model. Finally, the interfacial stress concentrations were quantified according to the stress concentration factor (SCF) by comparing local behaviors between the analytical model and experimental data.

4.1. Residual Stress Models Considering Thermally-induced Initial Damages

The thermally-induced initial damage due to the uneven cooling process after hot-rolling or welding can cause residual stresses in steel members. Figure 7 shows two residual stress models used in the sectional analysis to consider the thermally-induced initial damage. Conventional residual stress models due to hot-rolling are classified into a constant linear (developed by Galambos and Ketter (Galambos and Ketter 1959)), a linear (developed by the ECCS (1984)), and a parabolic (developed by Young (1972)) according to the stress distributions. For line A representing the behavior of the steel beams, the constant residual stress model was used as shown in Figure 7(a). A standardized residual stress model due to welding was presented by ECCS (1976), as shown in Figure 7(b). So, for line B representing the behavior of the connections, the ECCS residual stress model was used.

In the hot-rolling residual stress model, the compressive stress (σ_{RC}) and tensile stress (σ_{RT}) are calculated by equation (2) and equation (3), respectively. The tensile stress suggested in the ECCS model is equal to the yield stress. Since the line B is 30 mm away from the welded connections, the tensile stress can be less than the yield stress according to previous work (Long *et al*. 2009). So, in the welding residual stress model, considering the equilibrium condition, the compressive stress (σ_{WC}) and tensile stress (σ_{WT}) are determined as equation (4) and (5), respectively.

$$\sigma_{RC} = 0.3 f_y \tag{2}$$

$$\sigma_{RT} = \sigma_{RC} \frac{b_f t_f}{b_f t_f + t_w (h - 2t_f)} \tag{3}$$

$$\sigma_{WC} = 0.184 f_y \tag{4}$$

$$\sigma_{WT} = 0.735 f_y \tag{5}$$

Sectional analyses were performed for three models of no residual stress, hot-rolling residual stress, both hot-rolling and welding (i.e., welding) stress to evaluate the analytical moment-strain relationship without the interfacial stress concentration. The yield strength and yield strain

Table 1. Yield strength and yield strain obtained from sectional analysis

Model	Yield strength (kNm)	Yield strain (10^{-6} mm/mm)	Yielding location
No residual stress model	2118.4	1856	Top and bottom flange (tension and compression)
Hot-rolling residual stress model	1482.9	1301	Bottom flange (compression)
Welding residual stress model	561.6	493	Top flange (tension)

evaluated from the sectional analyses are summarized in Table 1. The yield strength of the DT-40 specimen is 623.5 kNm, the DT-45 specimen is 758.8 kNm, and the DT-50 specimen is 812.9 kNm, which are similar to the yield strength of the welding residual stress model. Also, the failure occurred the top flange after tensile yielding in all specimens. Since the welding residual stress model appropriately simulates the yield strength and yielding location of the specimens, the stress concentration factors are evaluated using the welding residual stress model.

4.2. Analytical Investigation of Stress Concentration Factors in Connections

The moment-strain curve derived using the welding residual stress model showed how the specimens would be expected to behave when there was no interfacial stress concentration on the connections. On the other hand, the moment-strain curve derived through experimentation showed how the specimens behaved when the connections were under the interfacial stress concentration. Therefore, in this study, the SCF for the connection between vertical through-plate and H-beam was quantified by comparing the strain measured experimentally and the analytical model results. In order to analyze the SCF according to the thickness of the vertical through-plate at the connection, the strain concentration factor (SNCF) was derived via equation (6). The SCF of the connection was evaluated using equation (7), which was developed

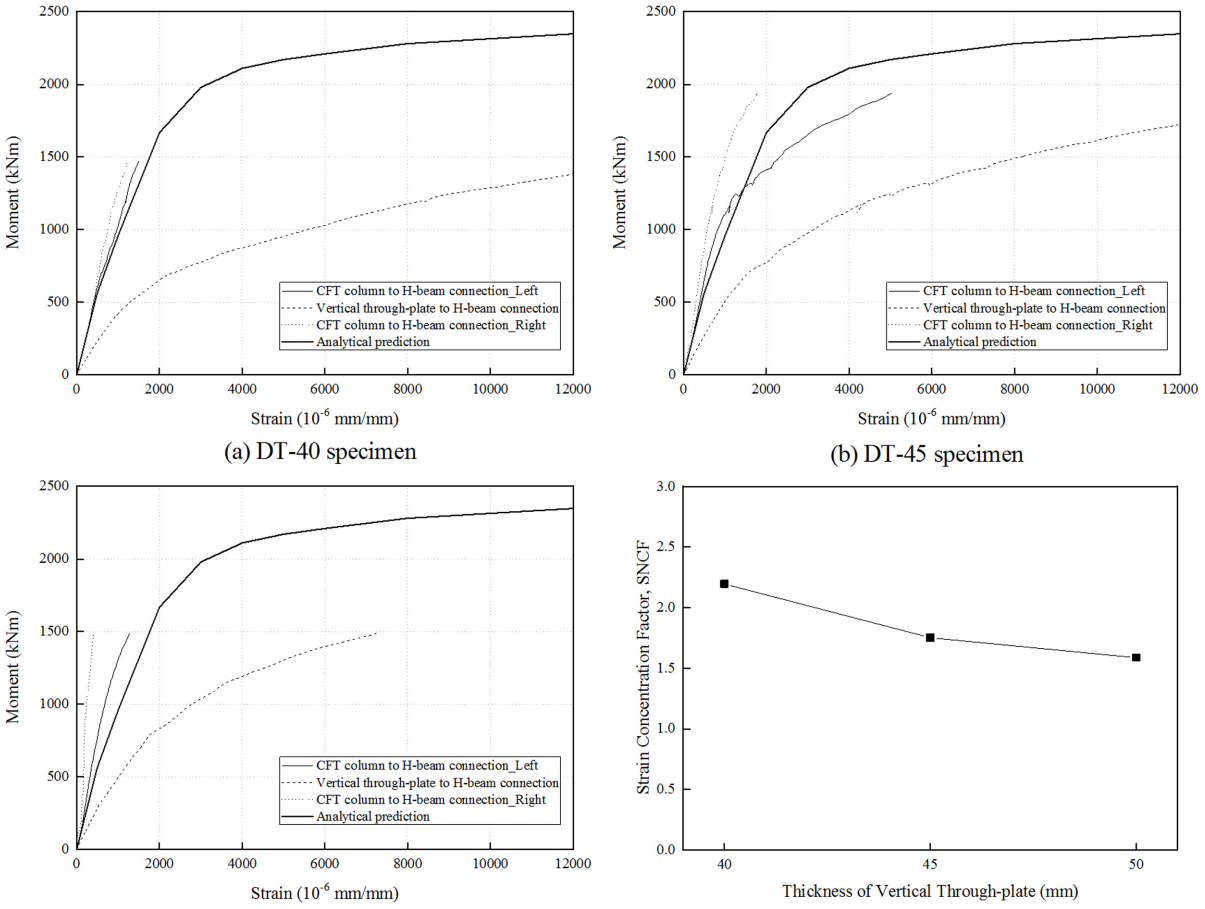


Figure 8. Comparison of experimental and analytical moment-strain curves and strain concentration factor in accordance with thickness of vertical through-plate.

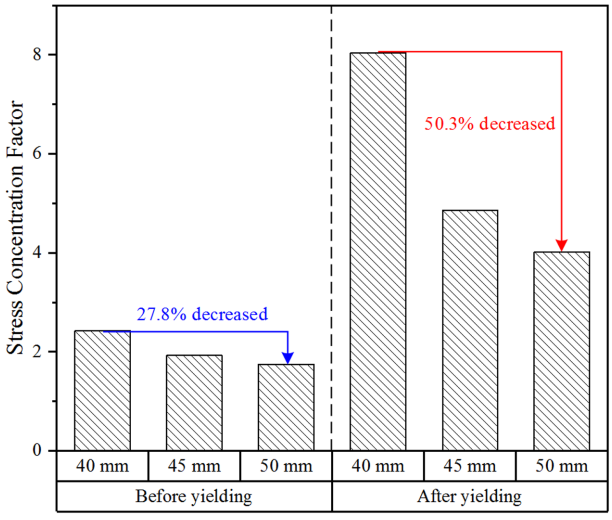


Figure 9. Stress concentration factor on the connection between vertical through-plate and H-beam according to the thickness of vertical through-plate.

from previous research (Chan *et al*. 2010; Musa *et al*. 2018).

$$SNCF = \frac{\varepsilon_E}{\varepsilon_A} \tag{6}$$

$$SCF = 1.2 \times SNCF \tag{7}$$

Where ε_E is experimental strain at the connection between vertical through-plate and H-beam and ε_A is analytical strain at the connection between vertical through-plate and H-beam.

Figure 8 shows a comparison of experimental and analytical moment-strain curves for all specimens. In Figure 8, the CFT column to H-beam connections mean the left and right sides of the line B, and the vertical through-plate to H-beam connections mean the center of the line B. The results showed that the analytical model appropriately simulates the initial behavior of the CFT column and H-beam connection. However, the behavior of the connection between the vertical through-plate and H-beam cannot be predicted well using the analytical model. This difference in the experimental and analytical strain can be considered as SNCF, and the SNCF at the yielding point is shown in Figure 8(d) according to the thickness of vertical through-plate. As the thickness of vertical through-plate increases, the SNCF tends to decrease, so the use of a thicker vertical through-plate will alleviate the strain concentration in the connection between the vertical through-plate and H-beam.

Figure 9 shows the SCFs for the connections between vertical through-plate and H-beam according to the thickness of vertical through-plate. The SCFs were evaluated before yielding (500 kNm) and after yielding (1200 kNm). The stress concentration on the connection with the vertical through-plate was positively correlated with load. The positive correlation between the stress concentration on the connection and load was also observed for the DT-45 and DT-50 specimens. The SCF for the connection between vertical through-plate and H-beam was negatively correlated the thickness of vertical through-plate. The SCF before yielding was 2.416 when the thickness of the vertical through-plate was 40 mm, 1.927 when the thickness was 45 mm, and 1.745 when the thickness was 50 mm. So, a thicker vertical through-plate can reduce the interfacial stress concentration on the center of the flange connected to the vertical through-plate. The SCFs after yielding were 8.045 when the thickness of the vertical through-plate was 40 mm, 4.862 when the thickness was 45 mm, and 4.002 when the thickness was 50 mm, respectively. So, the maximum reduction of the stress concentration factor due to an increase in the thickness of the vertical through-plate is 50.3%. When compared with those before yielding, as the load increased, the stress concentration on the connection between the vertical through-plate and H-beam decreased as the thickness of vertical through-plate increased. Therefore, thick vertical through-plate can be used to reduce interfacial stress concentration on the connections between vertical through-plate and H-beam in CFT columns.

5. Conclusions

In this study, the interfacial stress concentrations were evaluated for the connections between vertical through-plate to H-beam connections in CFT column. In order to investigate the thermally-induced initial damages in the connections, the residual stress models which best simulate the local behavior of the specimens were determined through sectional analyses. In addition, the stress concentration factors on the connections were quantified by comparing the local behavior of the connection between experiment and analysis. The following conclusions can be made from the findings of this study.

1. All specimens underwent brittle failure in the connection between the vertical through-plate and H-beam before reaching the theoretical maximum strength (2380.8kNm) of the steel beam. The experimental results showed that the interfacial stress concentrations at the center of the steel beam connected to the vertical through-plate were the main reason for the premature failure of the specimens.
2. In the moment-strain curve, the ratio of the initial slope of the steel beam and that of the theoretical initial slope are 0.931 to 1.132. However, the initial slope of the moment-strain curve at the connection with the vertical through-plate was 0.434 to 0.549 times lower than the theoretical initial slope. The early yielding induced by the residual stresses accelerated the interfacial stress concentrations of the connection between the vertical through-plate

and H-beam.

3. The welding residual stress model successfully simulated the moment-strain behavior of the connections in terms of the yield strength and yielding location. While the yield strengths evaluated by no residual stress and hot-rolling residual stress models were significantly larger than those of the specimens, the welding residual stress model can accurately estimate the yield strength of the specimens.
4. The stress concentration factor of the connection was evaluated from the difference in the strain of the experimental data that reflects the stress concentration effect and the analytical data that does not consider the stress concentration effect. As the thickness of the vertical through-plate increases from 40 mm to 50 mm, the stress concentration factors decrease from 8.045 to 4.002 representing a maximum reduction of 50.3%. This result suggests that the thick vertical through-plate can be applied to alleviate the interfacial stress concentration.

In conclusion, as the thickness of the vertical through-plate increases, the interfacial stress concentration on the connection decreases. However, since early yielding of the steel beam adjacent to the connection can be occurred due to the thermal damage caused by the welding of the thick vertical through-plate, there is a need to devise detailed measures capable of reducing the thermal damage due to welding in construction process.

Acknowledgments

This research was supported by a grant (NRF-2018 R1A2B6006958) from the National Research Foundation of Korea (NRF) funded by the Korean Ministry of Science and ICT (MSIT).

References

Abambres, M., Quach, W. M. (2016). "Residual stresses in steel members: A review of available analytical expressions." *Int. J. Struct. Integr.*, 7(1), 70-94.

Bu, Y., Gardner, L. (2019). "Finite element modelling and design of welded stainless steel I-section columns." *J. Constr. Steel Res.*, 152, 57-67.

Chan, J., Chen, J., Jin, W. L. (2010). "Experiment investigation of stress concentration factor of concrete-filled tubular T joints." *J. Constr. Steel Res.*, 66(12), 1510-1515.

Chen, C. C., Lin, C. C., Tsai, C. L. (2004). "Evaluation of reinforced connections between steel beams and box columns." *Eng. Struct.*, 26(13), 1889-1904.

Chen, M. cheng, Wen, Q. qing, Zhu, Q., Huang, H., Xie, L. (2017). "Simulation of corrosion process for concrete filled steel tubular columns with the cellular automata method." *Eng. Fail. Anal.*, 82, 298-307.

Choi, I., Kim, J. H., Kim, H.-R. (2015). "Composite Behavior of Insulated Concrete Sandwich Wall Panels Subjected to Wind Pressure and Suction." *Materials (Basel).*, 8, 1264-1282.

Choi, I., Kim, J. H., You, Y.-C. (2016). "Effect of cyclic loading on composite behavior of insulated concrete sandwich wall panels with GFRP shear connectors." *Compos. Part B Eng.*, 96, 7-19.

Choi, S., Lee, S., Hong, S., Kim, J. (2008). "Structural capacities of tension side for CFT square column-to-beam connections with combined-cross diaphragm." *Adv. Struct. Eng.*, 11(2), 209-227.

ECCS. (1976). *Manual on stability of steel structures - Part 2.2. Mechanical properties and residual stresses*. European Convention for Constructional Steelwork, Brussels.

ECCS. (1984). *Ultimate limit states calculations of sway frames with rigid joints*. European Convention for Constructional Steelwork, Brussels.

Galambos, T. V, Ketter, R. L. (1959). "Columns under combined bending and thrust." *J. Eng. Mech. Div.*, 85(2), 1-30.

Gardner, L., Bu, Y., Theofanous, M. (2016). "Laser-welded stainless steel I-sections: Residual stress measurements and column buckling tests." *Eng. Struct.*, 127, 536-548.

Gupta, P. K., Singh, H. (2014). "Numerical study of confinement in short concrete filled steel tube columns." *Lat. Am. J. Solids Struct.*, 11(8), 1445-1462.

Hajjar, J. F., Schiller, P. H., Molodan, A. (1998). "A distributed plasticity model for concrete-filled steel tube beam-columns with interlayer slip." *Eng. Struct.*, 20(8), 663-676.

Huang, C., Yeh, Y.-K., Liu, G.-Y., Hu, H.-T., Tsai, K., Weng, Y., Wang, S., Wu, M.-H. (2002). "Axial Load Behavior of Stiffened Concrete-Filled Steel Columns." *J. Struct. Eng.*, 128(9), 1222-1230.

Kang, L., Leon, R. T., Lu, X. (2014). "A general analytical model for steel beam-to-CFT column connections in OpenSEES." *J. Constr. Steel Res.*, 100, 82-96.

Kim, J. H., Ghaboussi, J., Elnashai, A. S. (2010). "Mechanical and informational modeling of steel beam-to-column connections." *Eng. Struct.*, 32(2), 449-458.

Kim, J. H., Ghaboussi, J., Elnashai, A. S. (2012). "Hysteretic mechanical–informational modeling of bolted steel frame connections." *Eng. Struct.*, 45, 1-11.

Kim, J. H., You, Y.-C. (2015). "Composite Behavior of a Novel Insulated Concrete Sandwich Wall Panel Reinforced with GFRP Shear Grids: Effects of Insulation Types." *Materials (Basel).*, 8, 899-913.

Kim, Y.-J., Shin, K.-J., Kim, W.-J. (2008). "Effect of Stiffener Details on Behavior of CFT Column-to-Beam Connections." *Steel Struct.*, 8(2), 119-133.

Kuranovas, A., Kvedaras, A. K. (2007). "Behaviour of hollow concrete?filled steel tubular composite elements." *J. Civ. Eng. Manag.*, 13(2), 131-141.

Lee, S. H., Yang, I.-S., Choi, S.-M. (2010). "Structural characteristics of welded built-up square CFT column-to-beam connections with external diaphragms." *Steel Compos. Struct.*, 10(3), 261-279.

Long, H., Gery, D., Carlier, A., Maropoulos, P. G. (2009). "Prediction of welding distortion in butt joint of thin plates." *Mater. Des.*, 30(10), 4126-4135.

Mirghaderi, S. R., Torabian, S., Keshavarzi, F. (2010). "I-beam to box-column connection by a vertical plate passing

through the column." *Eng. Struct.*, 32(8), 2034-2048.
Musa, I. A., Mashiri, F. R., Zhu, X., Tong, L. (2018). "Experimental stress concentration factor in concrete-filled steel tubular T-joints." *J. Constr. Steel Res.*, 150, 442-451.
Qin, Y., Chen, Z., Wang, X. (2014a). "Experimental investigation of new internal-diaphragm connections to CFT columns under cyclic loading." *J. Constr. Steel Res.*, 98, 35-44.
Qin, Y., Chen, Z., Wang, X., Zhou, T. (2014b). "Seismic behavior of through-diaphragm connections between CFRT columns and steel beams-experimental study." *Adv. Steel Constr.*, 10(3), 351-371.
Qin, Y., Chen, Z., Yang, Q., Shang, K. (2014c). "Experimental seismic behavior of through-diaphragm connections to concrete-filled rectangular steel tubular columns." *J. Constr. Steel Res.*, 93, 32-43.
Sakino, K., Nakahara, H., Morino, S., Nishiyama, I. (2004). "Behavior of Centrally Loaded Concrete-Filled Steel-Tube Short Columns." *J. Struct. Eng.*, 130(2), 180-188.
Samarakkody, D. I., Thambiratnam, D. P., Chan, T. H. T., Moragaspitiya, P. H. N. (2017). "Differential axial shortening and its effects in high rise buildings with composite concrete filled tube columns." *Constr. Build. Mater.*, 143, 659-672.
Sewel, J. S. (1902). "Column for Buildings." *Eng. News*, 48(17), 36-39.
Shin, K.-J., Kim, Y.-J., Oh, Y.-S., Moon, T.-S. (2004). "Behavior of welded CFT column to H-beam connections with external stiffeners." *Eng. Struct.*, 26(13), 1877-1887.
Srinivasan, C. N., Schneider, S. P. (1999). "Axially Loaded Concrete-Filled Steel Tubes." *J. Struct. Eng.*, 125(10), 1202-1206.
KATS. (2014). "Rolled steels for welded structures (KS D 3515)." Korean Agency for Technology and Standards.
Torabian, S., Mirghaderi, S. R., Keshavarzi, F. (2012). "Moment-connection between I-beam and built-up square column by a diagonal through plate." *J. Constr. Steel Res.*, 70, 385-401.
Xiao, Y., Zhang, Z., Hu, J., Kunnath, S. K., Guo, P. (2011). "Seismic Behavior of CFT Column and Steel Pile Footings." *J. Bridg. Eng.*, 16(5), 575-586.
Yang, B., Nie, S., Xiong, G., Hu, Y., Bai, J., Zhang, W., Dai, G. (2016). "Residual stresses in welded I-shaped sections fabricated from Q460GJ structural steel plates." *J. Constr. Steel Res.*, 122, 261-273.
Young, B., Ellobody, E. (2006). "Experimental investigation of concrete-filled cold-formed high strength stainless steel tube columns." *J. Constr. Steel Res.*, 62(5), 484-492.
Young, B. W. (1972). "Residual stresses in hot-rolled members." *IABSE Int. Colloq. column strength*, University of Cambridge.
Young, B. W., Schulz, G. W. (1977). "Mechanical properties and residual stresses." *Second Int. Colloqium Stab. Steel Struct. Liege Introd. Report, ECCS IABSE*.
Zeinizadeh Jeddi, M., Ramli Sulong, N. H., Arabnejad Khanouki, M. M. (2017). "Seismic performance of a new through rib stiffener beam connection to concrete-filled steel tubular columns: An experimental study." *Eng. Struct.*, 131, 477-491.